Atmósfera (1988), **1**, pp. 17-38

Possible causes and numerical simulation of the Northern Hemispheric climate during the last deglaciation

JULIAN ADEM *

Centro de Ciencias de la Atmósfera, Universidad Nacional Autónoma de Mézico, 04510, Mézico, D. F., MEXICO

(Manuscript received July 28, 1987; in final form October 20, 1987)

RESUMEN

Un modelo climático termodinámico se usa para simular en el Hemisferio Norte los climas de hace 18, 13, 10, 7 y 4 mil años hasta el presente.

Las computaciones muestran la gran importancia en el ciclo anual del clima, de las anomalías de la insolación debidas a las variaciones de la órbita terrestre, especialmente para el período más reciente desde hace más o menos 12 mil años hasta el presente, en que los promedios de las anomalías mensuales de temperatura superficial calculadas para el Hemisferio Norte muestran el mismo patrón de signos que las anomalías de insolación, excepto por un retraso asociado con el almacenamiento de calor en los océanos.

Se demuestra que en el período de 18 a 12 mil años antes del presente el efecto de retroalimentación del albedo de superficie debido a la presencia de capas de hielo, mantuvo negativo el valor promedio mensual de las anomalías de temperatura en la superficie durante todo el año, ocurriendo el efecto máximo para hace 18 mil años. El efecto de las variaciones orbitales fue producir mayores variaciones estacionales en la temperatura superficial, asociadas con las anomalías de la insolación, a pesar de que el promedio anual de éstas es insignificante. El efecto de la disminución del CO_2 atmosférico fue incrementar la magnitud de la anomalía negativa de la temperatura superficial.

La magnitud promedio de las anomalías calculadas de la temperatura superficial del océano para hace 18 mil años, es como dos tercios del valor estimado por CLIMAP (1976). Dichas anomalías se deben al efecto combinado de la existencia de las capas de hielo, la disminución de CO_2 atmosférico y las anomalías de insolación.

ABSTRACT

A thermodynamic climate model is used to simulate the Northern Hemisphere climates for 18, 13, 10, 7 and 4 kyr BP, and to evaluate the importance of the ice sheets, the insolation anomalies and the variation of the atmospheric CO_2 in the maintainance and evolution of the terrestrial climates from 18 kyr BP to present time.

The computations show the great importance of the insolation anomalies, due to orbital variations, in the annual cycle of climate, especially for the most recent period from about 12 kyr BP to present time, when the computed monthly average Northern Hemisphere surface temperature anomalies have the pattern of negative and positive anomalies shown in the insolation anomalies, except for a lag associated with the storage of heat in the oceans.

It is shown that from 18 to 12 kyr BP the surface albedo feedback effect, due to the presence of ice sheets, maintains the average Northern Hemisphere surface temperature anomalies negative through the whole year, having its maximum effect at 18 kyr BP. The effect of the orbital variation is to produce larger seasonal variations in the surface temperatures, associated with the variations of the insolation anomalies which are non-negligible despite the fact that their annual average is negligible. The effect of the decrease of the atmospheric CO_2 is to reinforce the negative anomalies of the surface temperature.

The average of the computed surface ocean temperature anomalies for 18 kyr BP, is about two thirds of the value estimated by CLIMAP (1976), and is due to the combined effect of the existance of the ice sheets, the decrease of atmospheric CO_2 and the anomalies of insolation, as external forcings.

1. Introduction

Several studies have been carried out on the simulation of climate for 18 000 years ago, when the maximum recent glaciation ocurred (Gates, 1976 a, b; William *et al.*, 1974; Manabe and Hahn, 1977; Alyea, 1972; Newell and Herman, 1975; Saltzman and Vernekar, 1975; Adem, 1981 a, b; Kutzbach and Wright, 1985).

---

*Member of "EL COLEGIO NACIONAL"

The simulation with numerical models of the climates during the deglaciation period from 18 kyr BP to present, have also been the subject of some papers, which include those of Kutzbach and Otto-Bliesner (1982); Swain, *et al.* (1983); Kutzbach (1983 a, b); Kutzbach and Guetter (1984 a, b); Hastenrath and Kutzbach (1985); Kutzbach and Street-Perrot (1985); Winkler *et al.* (1986); Kutzbach and Guetter (1986), and Adem *et al.* (1984).

In all these papers the ocean temperature has been prescribed. Recently the author (Adem, 1985) published a simulation of the climate of 10 kyr BP in which the ocean temperature is carried out as a variable, as well as the snow-ice boundary, using the so called thermodynamic model, described in recent papers (Adem 1982; Adem and Garduño, 1984).

The purpose of this paper is to carry out simulations of climate, similar to the one above mentioned for 10 kyr BP, for other periods of time during the last deglaciation. The numerical experiments will include, besides 10 kyr BP, the simulations of climate for 18, 13, 7 and 4 kyr BP. The results will be used to deduce the long-term evolution of climate during the last 18 000 years, as well as to evaluate the contribution of the different possible causes responsible for maintaining the types of climate that existed during such period of time.

2. The model and the data used

The model used in these experiments is described by Adem (1982) which, as in the experiments for 10 kyr BP (Adem, 1985) has been modified so that the conservation of water vapor is satisfied. The version of the model used is the one of experiment 3 in Adem and Garduño (1984).

Furthermore, the effect of the decrease of the atmospheric CO_2 will be included, using the method described by Adem and Garduño (1982, 1984). Therefore, for information about the detailed characteristics of the model used, the reader is refered to these papers.

The model is hemispheric, the equations and variables are monthly averages, the time step is of one month, and the solution is obtained after about 8 years of integration and is obtained as a set of monthly charts for the following variables: the surface (ground) temperature in continents, the sea surface temperature anomalies, the mid-tropospheric temperature, the heating by short and long-wave radiation, and the horizontal heat transport by mean wind and transient eddies. The model also includes as variables computed internally: the anomalies of evaporation at the surface, sensible heat given off from the surface to the atmosphere, and heat gained by condensation of water vapor in the clouds.

The surface albedo is also carried out as variable by adjusting in each time step the boundary of snow and ice so that it coincides with the computed 0^oC surface isotherm, in the way described in detail by Adem (1981a).

The region of integration and the grid points are shown in Fig.1

As in all the previous simulations, the method used is to simulate first the climate of present-day conditions, and then the climate associated with the conditions that existed during the period considered. The computed "anomalies" of the climatic variables are estimated substracting from these the corresponding computed variables for present day conditions.

In the numerical experiments, three factors are postulated as the possible causes of the evolution of climate from the last great glaciation, 18 000 years ago, to present. Such factors are: The extent of the ice sheets, the insolation changes due to orbital variations and the atmospheric CO_2 content.

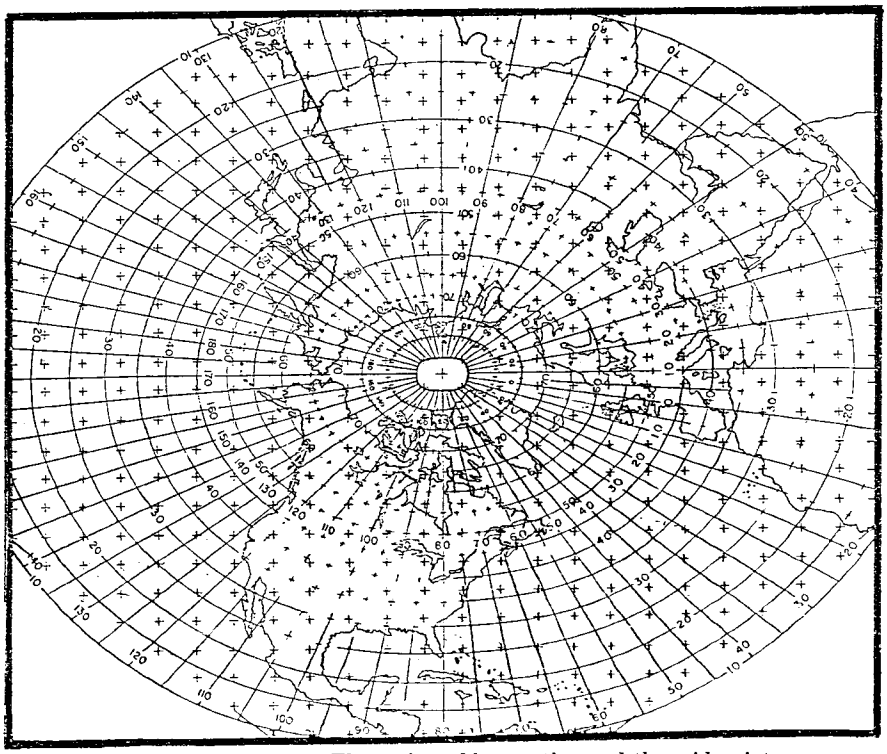

Figure 1. The region of integration and the grid points.

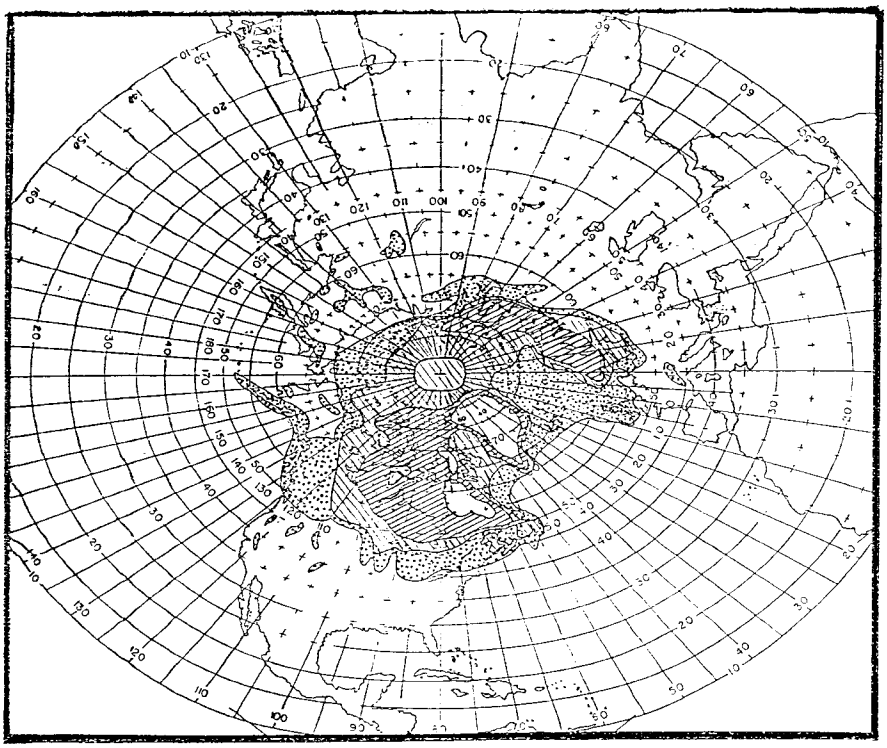

Figure 2. The ice sheets extents for 18, 13, 10 and 7 kyr BP (Denton and Hughes, 1981). Ablation from 18 to 13 kyr BP: dotted shading; from 13 to 10 kyr BP: -45° slope lines shading; and from 10 to 7 kyr BP: 45° slpe lines shading.

Ice sheets

Fig. 2 shows the ice sheet extents as given by Denton and Hughes (1981), for 18, 13, 10 and 7 kyr BP.

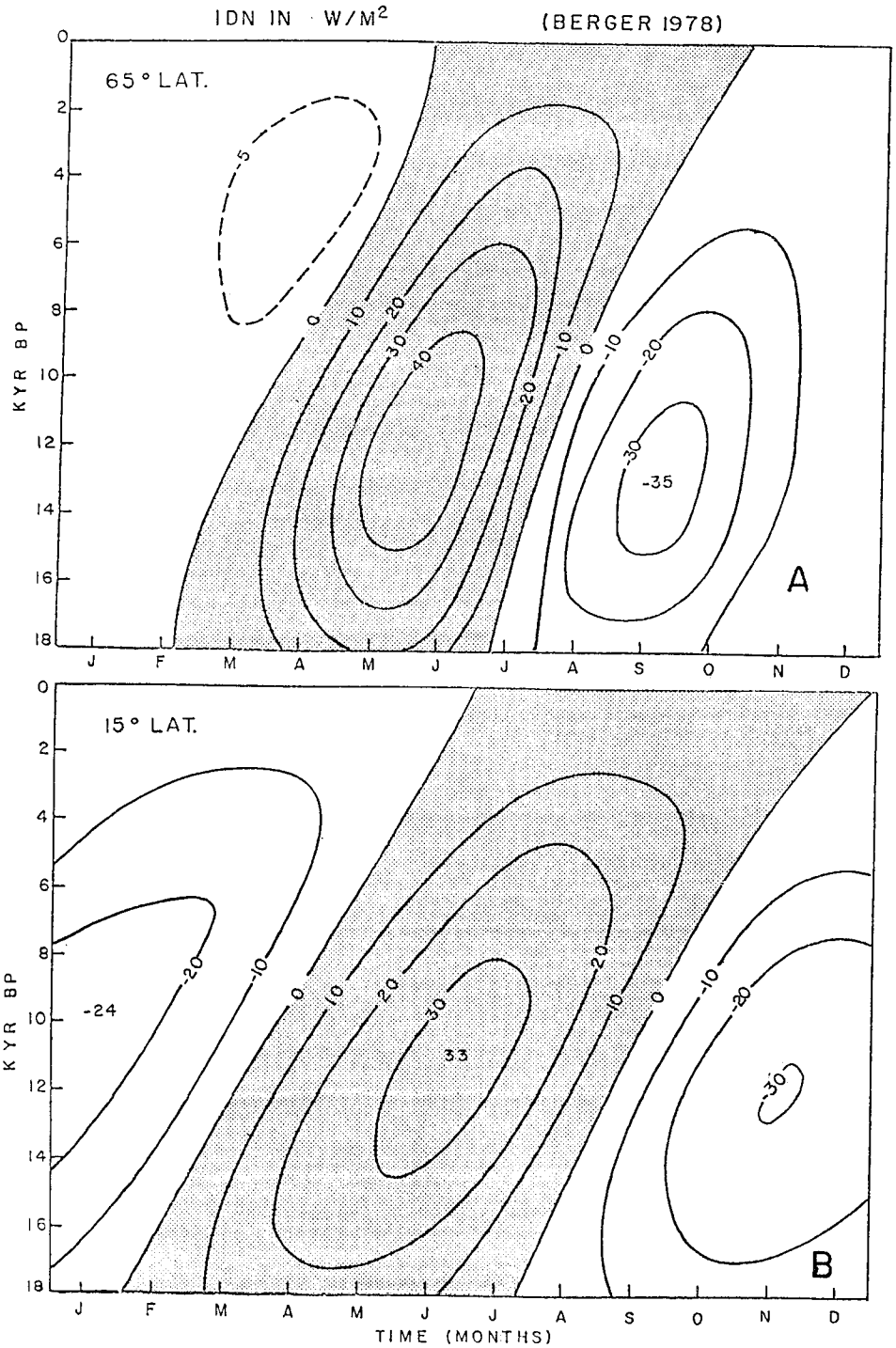

Figure 3. The mean monthly isolation departures from present values in Wm^{-2}, for the period from 18 kyr BP to present, for 65° Lat. (Part A), and 15° Lat. (Part B). (Berger. 1978).

The area with dotted shading is the ablation from 18 to 13 kyr BP; the area shaded with -45^o slope lines is the ablation from 13 to 10 kyr BP, and the area shaded with 45^o slope lines is the ablation from 10 to 7 kyr BP.

Insolation anomalies due to orbital variations

The mean monthly insolation departures from present values as given by Berger (1978) will be used in the computations. In Fig. 3 are shown these values for 65^o latitude (Part A) and 15^o latitude (Part B). The ordinate is the time in kyr BP, and the abscissa the time of the year in months. The figure shows the isolines of the insolation departures from present values in Wm^{-2}. The shaded area corresponds to positive values. For other latitudes the pattern is similar, showing that for the whole period the values are negative during five to six consecutive months and then become positive during the rest of the year. The position of the change of sign and the magnitude is shown in a clear way in Fig. 3.

Variation of CO_2

Fig. 4 shows the atmospheric CO_2 level reconstructed by Neftel *et al.* (1982) from ice core measurements. This figure shows that the concentration of CO_2 during 18 kyr BP was about 26 percent smaller than at present, and since then, as the ice sheets retreated, it increased reaching the present level of CO_2 concentration at about 8 kyr BP.

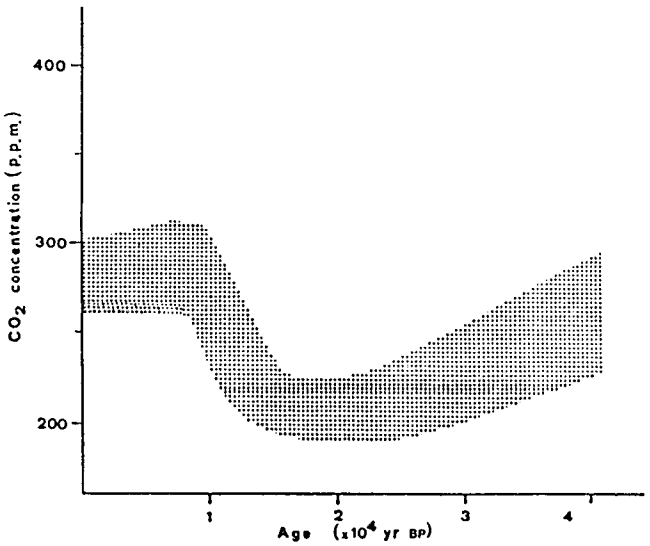

Figure 4. The atmospheric CO_2 concentration from 40 kyr BP to present (Neftel, *et al.* 1982).

3. The numerical experiments

Using the model and the data mentioned above, the simulations of climate for 18, 13, 7 and 4 have been carried out. The present days ice sheets extent is used for 4 kyr BP.

Although the model yields all the variables mentioned in the previous section, only the computed

surface temperature departures from present values will be shown, and will be denoted T_sDN, and refered as "departures" or "anomalies".

Parts A, B, C and D of Fig. 5 show T_sDN, in tenths of Celsius degrees for July at 18, 13, 7 and 4 kyr BP respectively.

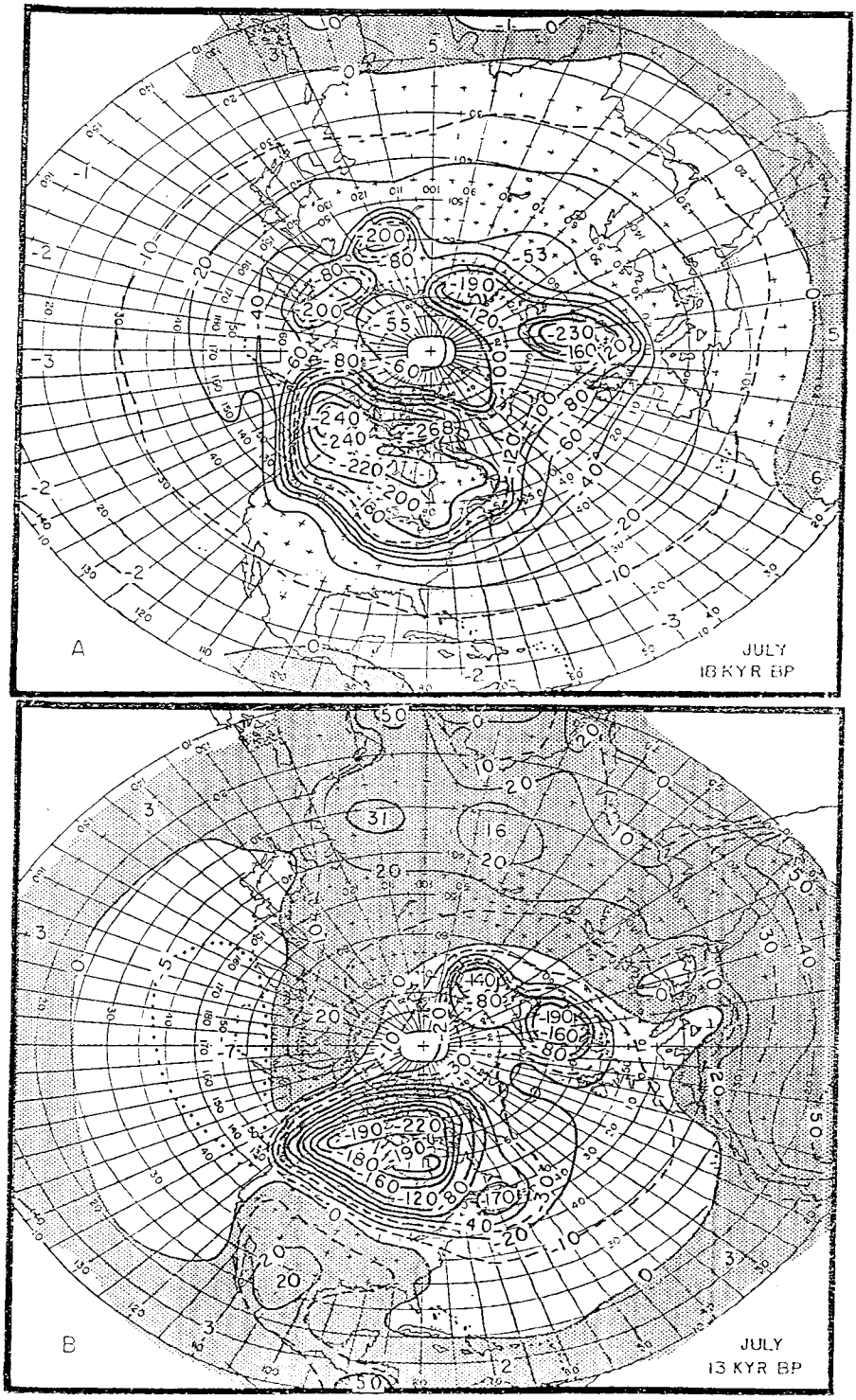

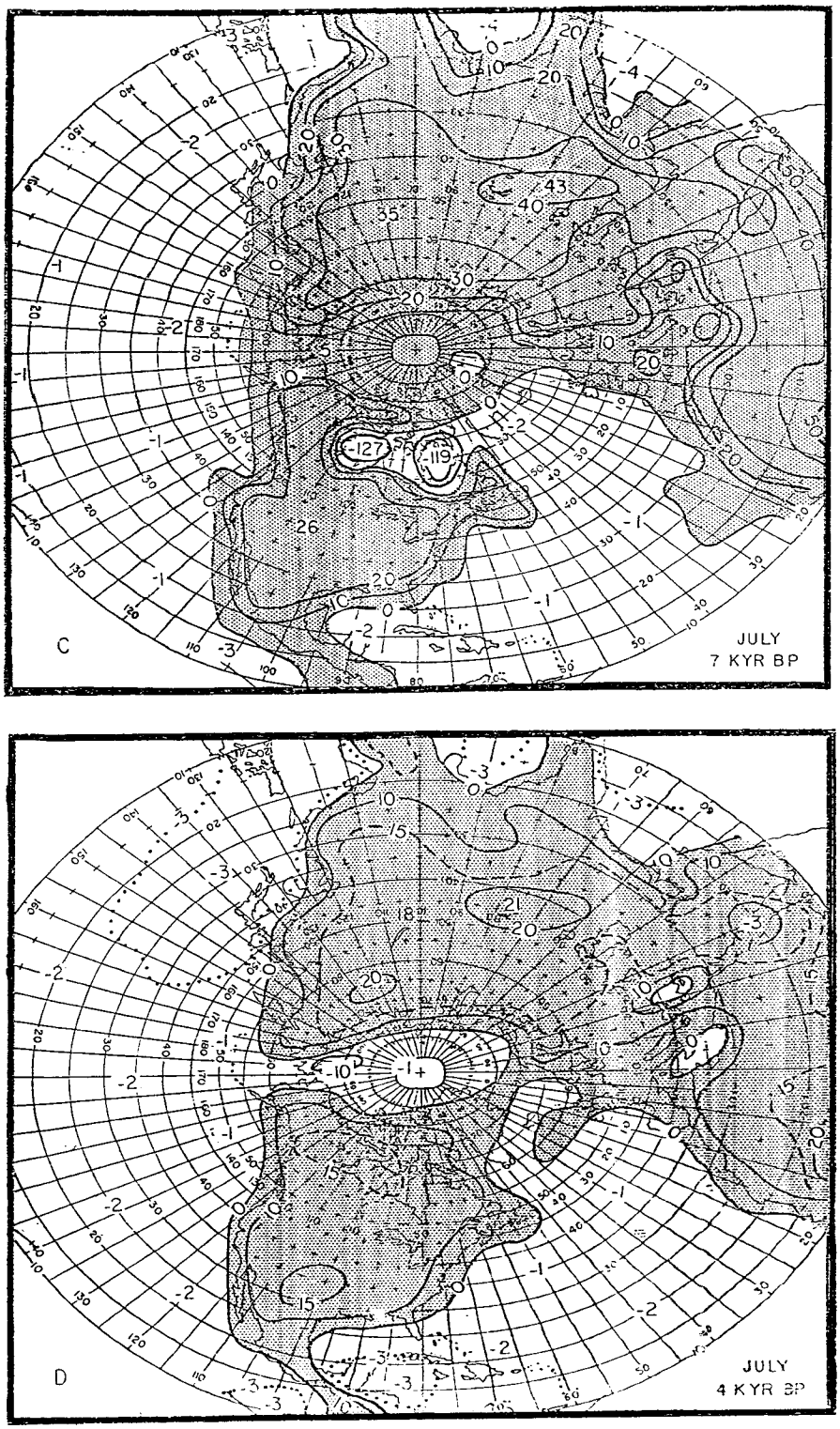

Figure 5. July surface temperature departures from present values, in tenths of Celsius degrees, Parts A, B, C and D correspond to 18, 13, 7 and 4 kyr BP respectively.

This figure shows the strong negative departures due to the snow-ice anomalies, which decrease towards the present time; and the positive anomalies over the continents, associated with the insolation anomalies and which have their maximum at the middle of the deglaciation period.

Fig. 6 is similar to Fig. 5 but for January. In this case the departures are negative, and decrease towards the present time.

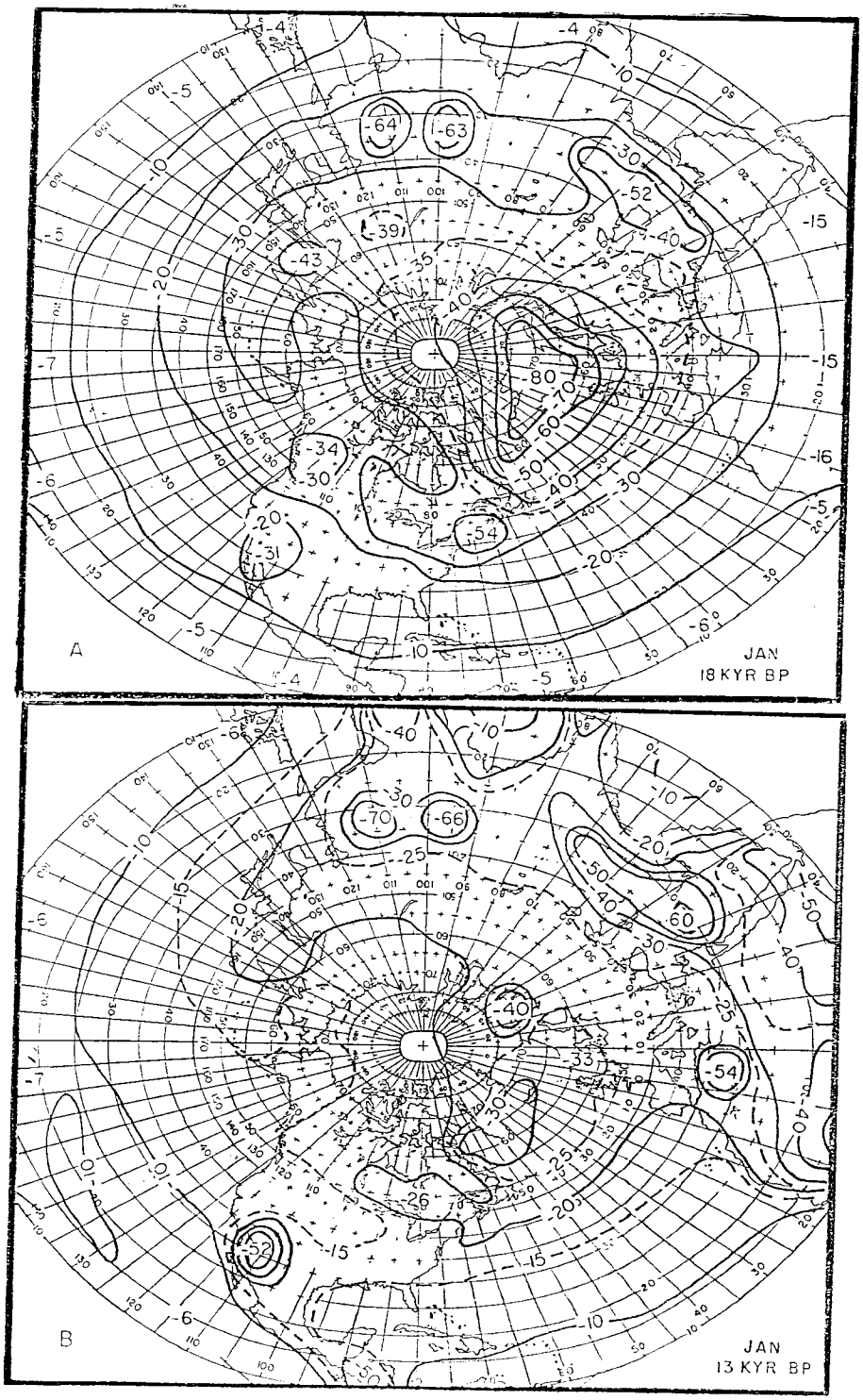

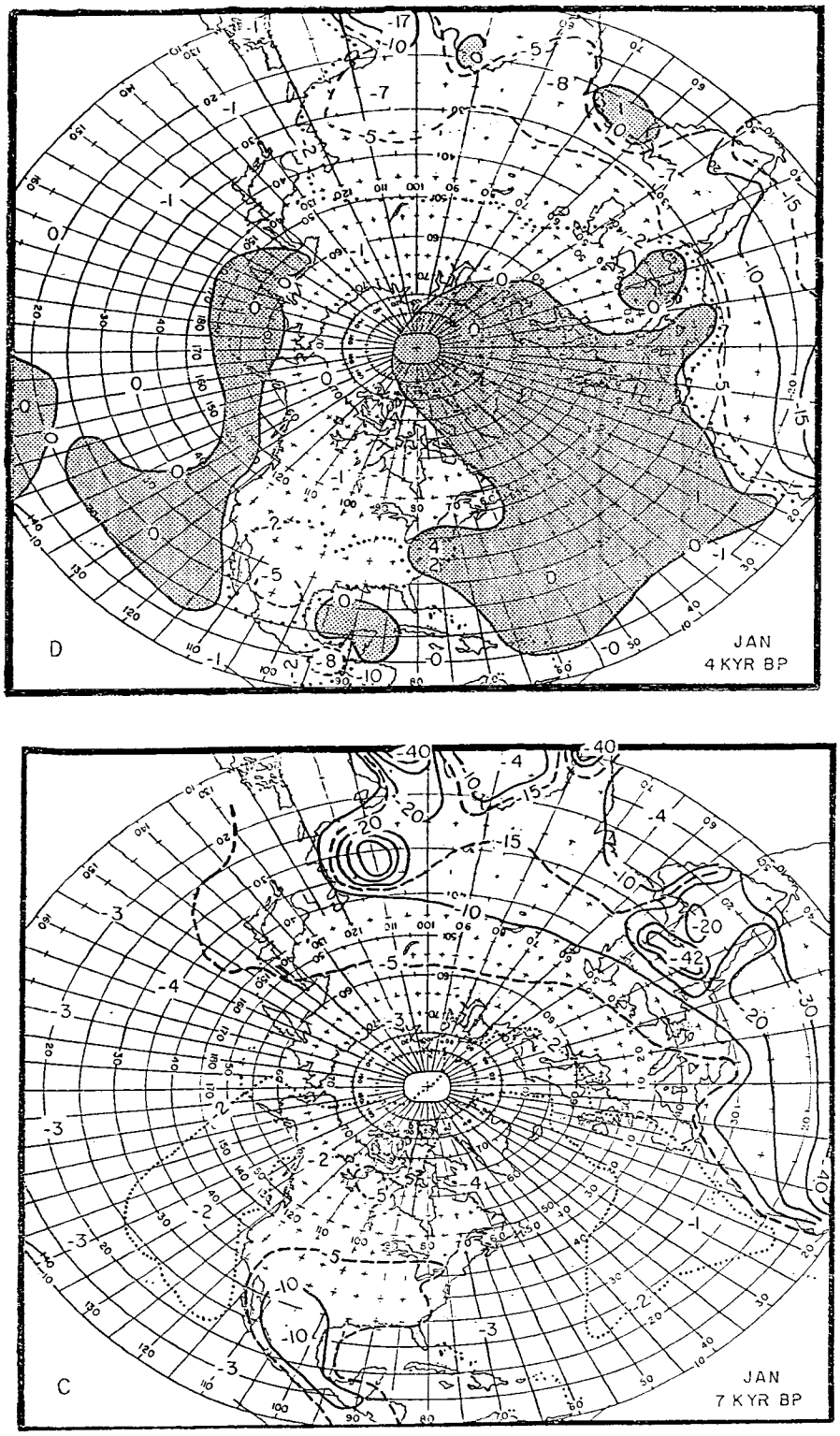

Figure 6. January surface temperature departures from present values, in tenths of Celsius degrees. Parts A, B. C and D correspond to 18, 13, 7 and 4 kyr BP respectively.

In order to study the evolution of climate and the impact of the different factors, during the last deglaciation, it is helpful to consider the average values over the whole region of integration, which is shown in Fig. 1. Despite the fact that the boundary of the integration region is at about 10^o of latitude, this average will be considered as representative for the Northern Hemisphere (N. H.).

Fig. 7 shows such averages for the insolation anomalies, given by Berger (1978). In this figure lines of equal insolation anomalies are shown in watts per square meter (Wm^{-2}). The abscissa is the time of the year in months and the ordinate the time before present in thousand of years (kyr BP).

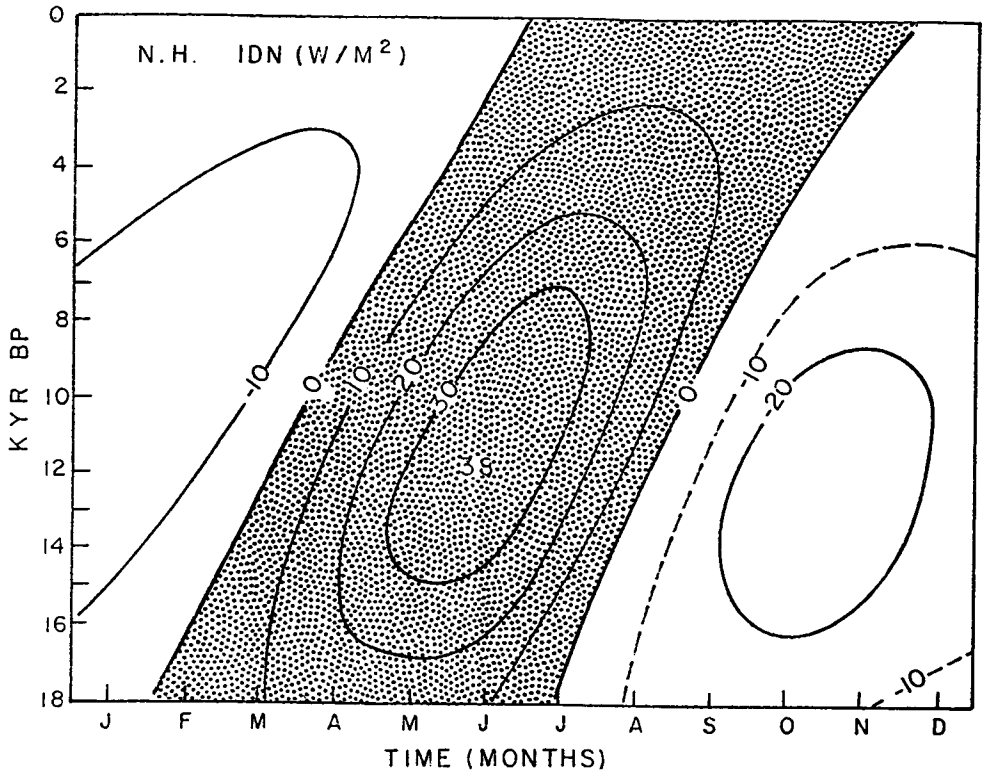

Figure 7. Average, over the total integration region, of the insolation departures from present values. Lines of equal departures are shown in Wm^{-2}. The abscissa is that time of the year in months and the ordinate the time before present in thousand of years.

In this figure the shaded area corresponds to positive values, showing a similar pattern as Fig. 3.

Fig. 8 shows the computed Northern Hemisphere average T_sDN. The abscissa is the time of the year in months and the ordinate the time in kyr BP. The figure shows isotherms in Celsius degrees.

Fig. 9 is as Fig. 8 except that it shows the average temperature over the grid points in the continents. It shows a similar pattern as Fig. 8, but with larger values. The largest negative value is in August of 18 kyr BP and is equal to about -5.0^oC and the largest positive value is in the Summer of 7 kyr BP and is equal to 2.7^oC.

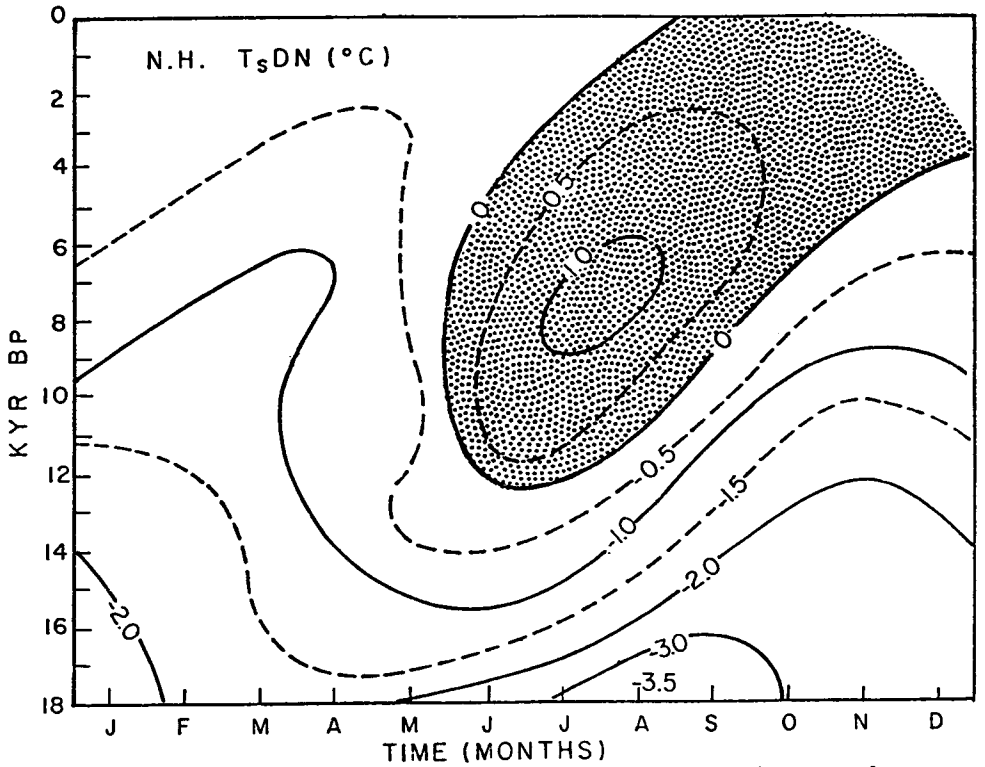

Figure 8. Average, over the total integration region, of the computed surface temperature departures from present values. Lines of equal departures are shown in tenths of Celsius degrees. The abscissa is the time of the year in months and the ordinate the time before present in thousand of years.

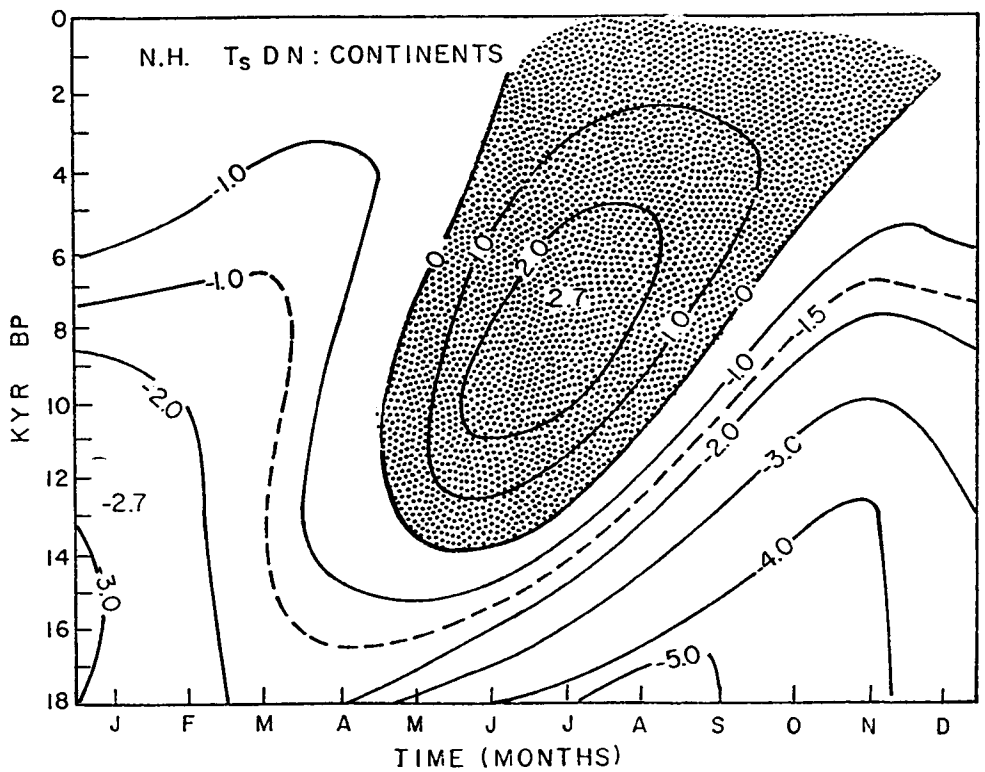

Figure 9. Same as Fig. 8, but average over continents in the total integration region of the computed surface ground temperature departures from present values.

Fig. 10 shows the computed Northern Hemisphere surface ocean temperature anomalies. From 18 to 10 kyr BP it remains negative, with a maximum negative value of -2.0^{o}C in the Fall of 18 kyr BP.

From 10 kyr to present it shows the pattern of changing from negative to positive anomalies in the annual cycle, as the continental temperature anomalies, but with a larger lag with respect to the insolation anomalies. For this period the absolute value of the anomalies is smaller than 0.5^{o}C.

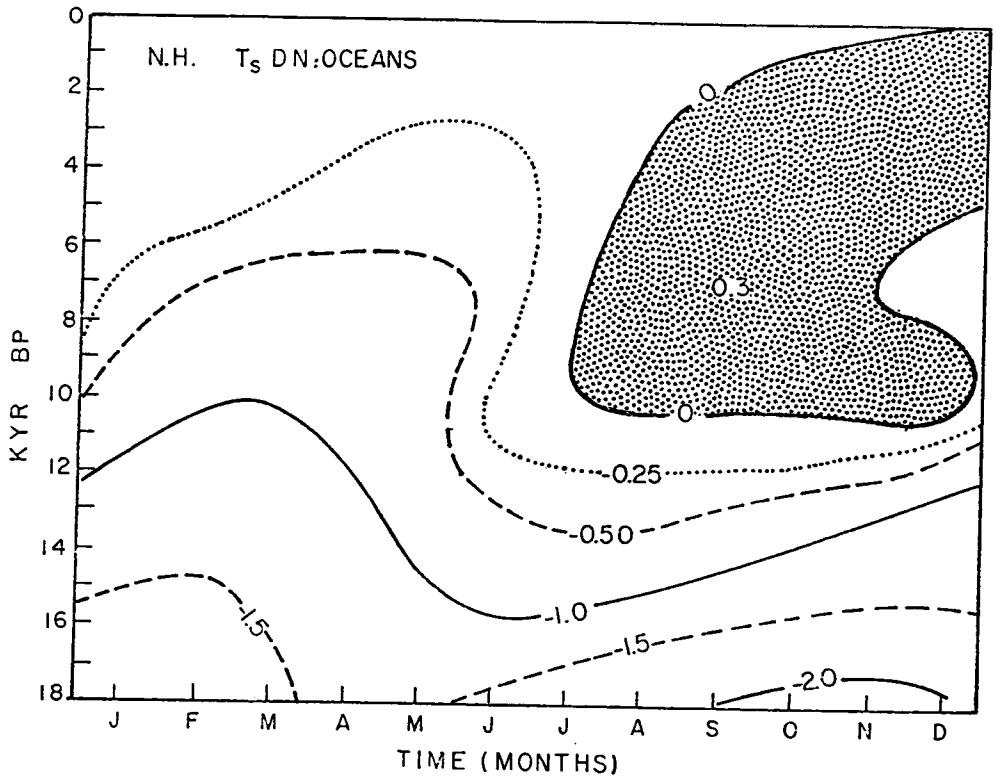

Figure 10. Same as Fig. 8, but average in the total integration region of the sea surface temperature departures from present values.

Fig. 11 shows the annual averages of T_sDN, as a function of time. The ordinate is the annual average of T_sDN in Celsius degrees and the abscissa the time, in kyr BP. The continuous curve corresponds to the average value of T_sDN over the Northern Hemisphere. The dashed and dotted curves correspond to the average values of T_sDN over the continents and oceans repectively. This figure shows that the annual N. H. average of T_sDN is negative from 18 to 4 kyr BP, and is equal to zero from 4 kyr to present. The values of T_sDN are equal to -2.5, -1.3, -0.6, -0.2, at 18, 13, 10 and 7 kyr BP respectively.

The dashed curve shows that the annual average over the continents (T_{s_c}DN) is equal to -3.7, -1.8, -0.7, -0.1 and 0.1 for 18, 13, 10, 7 and 4 kyr BP respectively. This curve also shows that T_{s_c}DN is positive after 6.5 kyr BP with a maximum value of 0.1 at 4 kyr BP.

The annual average of the surface ocean temperature, T_{s_0}DN, (dotted curve) is negative over the whole period of deglaciation, with values equal to -1.8, -0.9, -0.3, -0.2, -0.1 for 18, 13, 10, 7 and 4 kyr BP respectively.

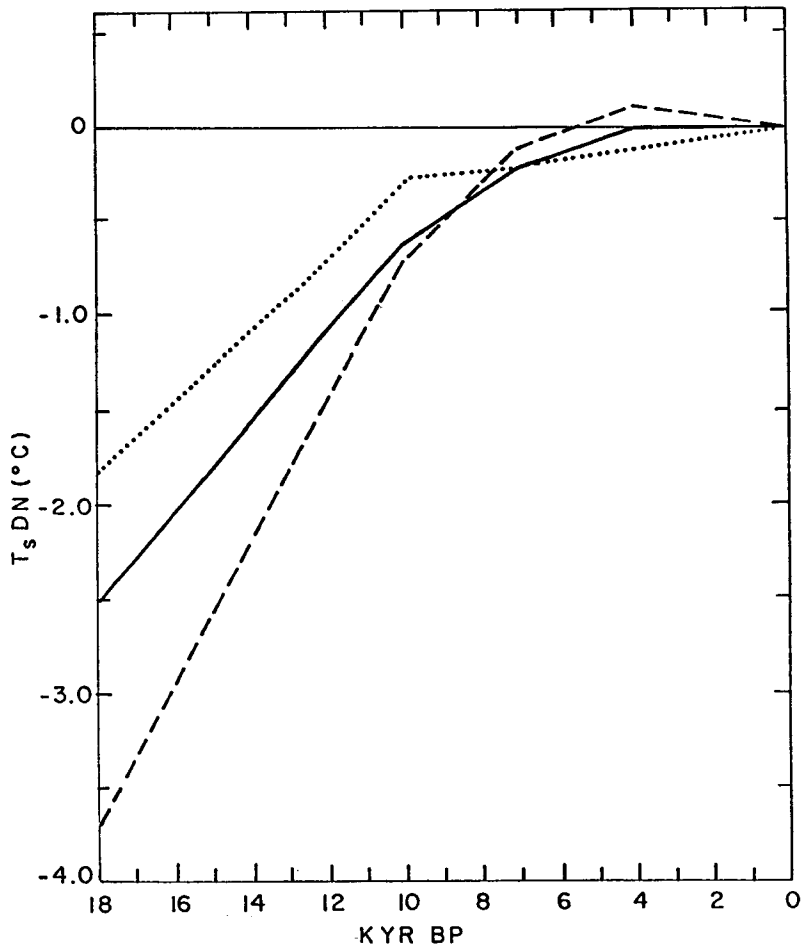

Figure 11. The annual average of the surface ground temperature departures from present values for the period from 18 kyr BP to present. The continuous line corresponds to the average over the Northern Hemisphere. The dashed and dotted lines correspond to the average continental ground temperature departures and the average sea surface temperature departures, respectively.

4. The contributions of the orbital variations, the ice sheets, and the decrease of CO_2

A comparison of Fig. 8 with Fig. 7 shows the great importance of the insolation anomalies, due to orbital variations, in the evolution of the average surface temperature, and of its annual cycle especially for the most recent period from about 12 kyr BP to present time. During this period the temperature anomalies have the pattern of negative and positive shown in the insolation anomalies, except for a lag, associated with the storage of heat in the oceans (Adem, 1985). The maximum positive value occured in Summer at 7 kyr BP and was of 1.0°C.

For the period from 18 to 12 kyr BP the surface albedo feedback effect due to the presence of ice sheets, maintains the average N. H. surface temperature anomalies negative through the whole year, having its maximum effect at 18 kyr BP, with the largest negative value of -3.5° in August of this millenium. However, the comparison of Fig. 8 with Fig. 7 shows that during this period the insolation effect is also important.

In a previous paper (Adem, 1985) a comparative study of the relative importance of the insolation anomalies and the ice sheets for 10 kyr BP has been carried out. A comparison of the effect of these two factors, as well as of the decrease of CO_2 will be presented in this section, specially for 18 kyr BP.

Fig. 12 shows the computed surface albedo anomalies (A) and the computed surface temperature anomalies (B), as functions of latitude, for July (continuous line) and January (dashed line) for 18 kyr BP. This figure shows that the anomalies of surface albedo (which correspond to the anomalies of snow and ice) are strongly correlated with the negative anomaly. This result is due to the feedback mechanism between the snow-ice cap and the surface temperature.

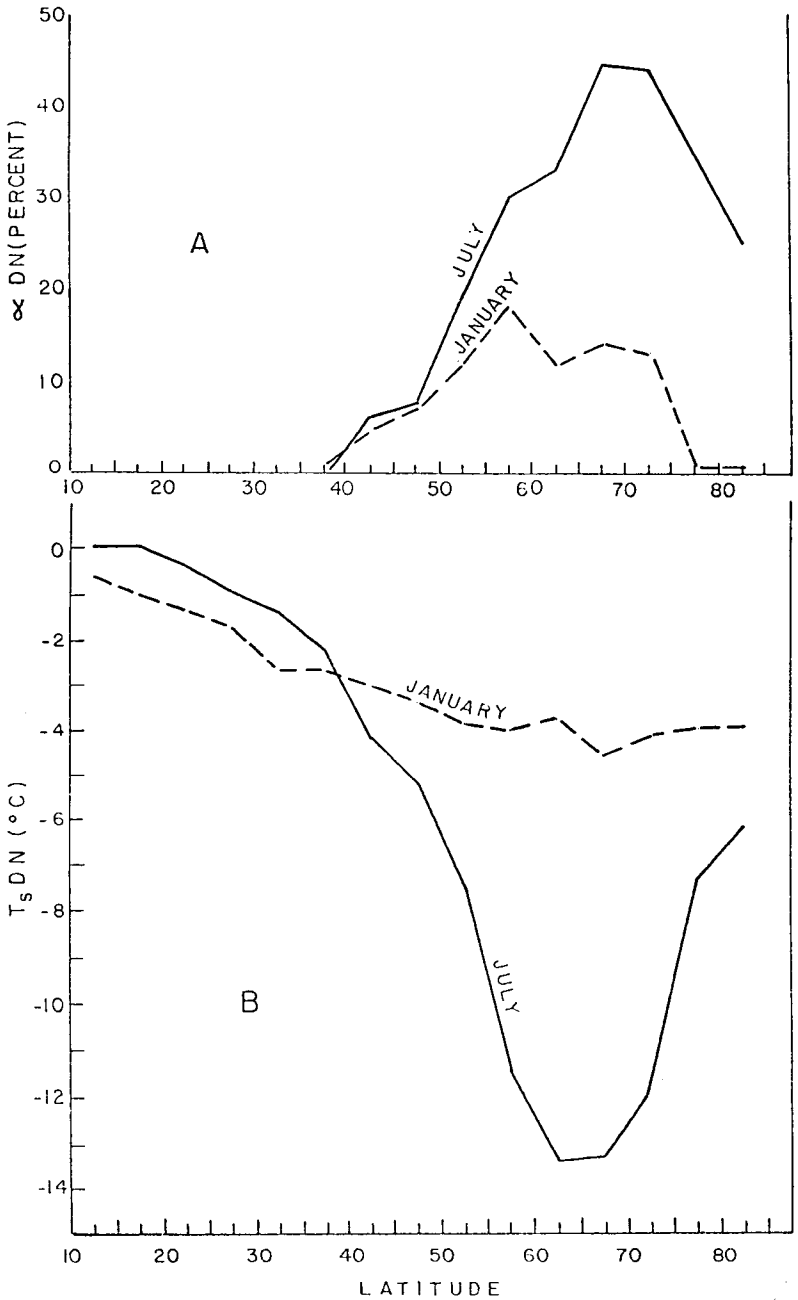

Figure 12. The computed 18 kyr BP surface albedo anomalies (Part a), and surface temperature anomalies (Part B), as a function of latitude, for July (continuous line) and January (dashed line).

Fig. 13 shows in parts A, B and C, the average of the anomalies in the Northern Hemisphere for 18 kyr BP of insolation (IDN), surface temperature (T_sDN) and surface albedo (α DN) respectively. The abscissa is the time of the year in months. The ordinate, in parts A, B and C is in watts per square meter, Celsius degrees, and percent, respectively.

In 13B and 13C the continuous lines correspond to the solution when Berger's (1978) values of IDN are used, and the dashed line to the solution when IDN is neglected, which correspond to using present values of insolation. A comparison of the continuous and dashed curves in 13B shows that the effect of IDN is to produce a climate with stronger seasonal variations, with respect to the present climate, by decreasing the negative anomalies of temperature in Spring and Summer and increasing them in the Fall and Winter. This effect is slightly accentuated by a small decrease of the surface albedo in Spring and Summer and by an increase in Fall and Winter, shown in Fig. 13C, and due to the temperature snow-ice feedback effect.

In the cases represented by the continuous and dashed lines, besides the ice sheets, the decrease of atmospheric CO_2 has been used. The dotted curve in 13B corresponds to the case when the effect of the decrease of the atmospheric CO_2 has been neglected, and only the effects of the ice sheets and the insolation anomalies have been included. Comparison of this curve with the continuous one, shows that the effect of the decrease of CO_2 is to decrease the surface temperature an average of about 0.4^oC in the Northern Hemisphere. Fig. 13B also shows that the anomalies of the surface temperature 18 000 years ago, were mainly due to the existence of the surface ice sheets and the anomalies of snow that existed through the year, but the other two factors had the non-negligible effects mentioned above.

It is of interest to compute the effect of the three parameters in the oceans and continents. Fig. 14 is similar to Fig. 13B but for the N. H. average surface ocean temperature (part A) and the N. H. average surface continental ground temperature (part B). It is clear from this figure that the response to the three parameters is much stronger in the continents than in the oceans.

Fig. 15 shows the net effect of the anomalies of the insolation (part A) and of the atmospheric CO_2 decrease (part B). The continuous, dashed and dotted lines correspond to the average increase of the surface temperature anomalies for the N. H., the N. H. continents and N. H. oceans, respectively.

The dashed curve of Fig. 15A shows that the net effect of the insolation in the continents is to decrease the magnitude of the negative anomaly of the ground temperature from March to July, with a maximum value of 1.7^oC in May, and increase it from August to February with a maximum value of 1.3^oC in September, October and November.

The dotted curve of 15A shows that, in the oceans; the net effect is to decrease the magnitude of the negative surface ocean temperature from April to September, with a maximum of 0.4^oC in June and July, and to increase it from October to March, with a maximum of 0.3^oC in January. The net effect in the average for the Northern Hemisphere, is a decrease of the magnitude of the negative anomaly from March to July, with a maximum of 1.0^oC in June, and an increase from August to February, with a maximum of 0.6^oC in November.

A comparison of 15A with 13A shows that there is a strong positive correlation between the insolation anomaly and its net effect in the surface temperature anomaly, except that in the average for the continents there is a lag of about 1/2 month, and for the oceans a lag of about two months.

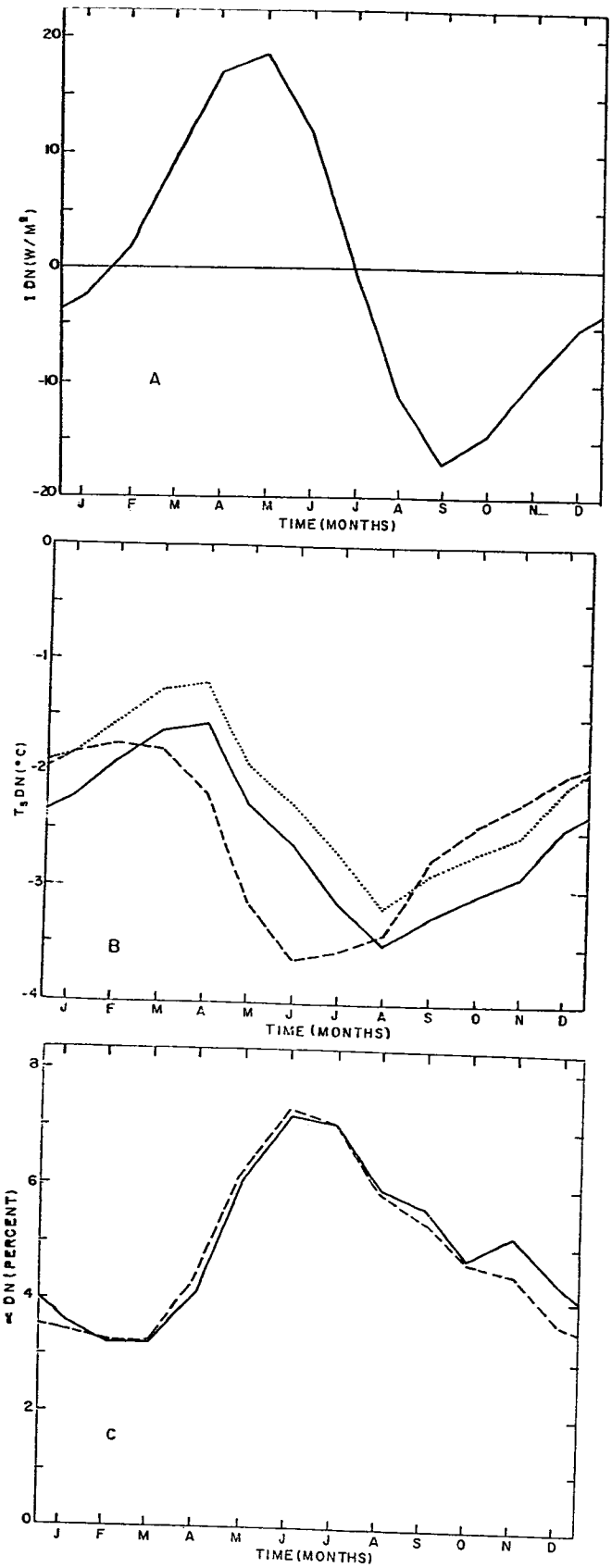

Figure 13. The continuous lines are the average N. H. anomalies for 18 kyr BP of insolation (Part A), computed surface temperature (Part B) and computed surface albedo (Part C). Dashed lines in B and C correspond to the case when the insolation anomalies (shown in A) are taken equal to zero. Teh dotted line corresponds to the case when the decrease of CO_2 has been neglected.

For the average in both oceans and continents the lag is of about one month. This lag effect is due to the storage of heat in the oceans. A detailed study of the effect of this storage of heat, as a function of the depth of the ocean mixed layer has been carried out for the case of 10 kyr BP (Adem 1985).

It is interesting to notice that despite the fact that the annual averages of the anomaly of insolation

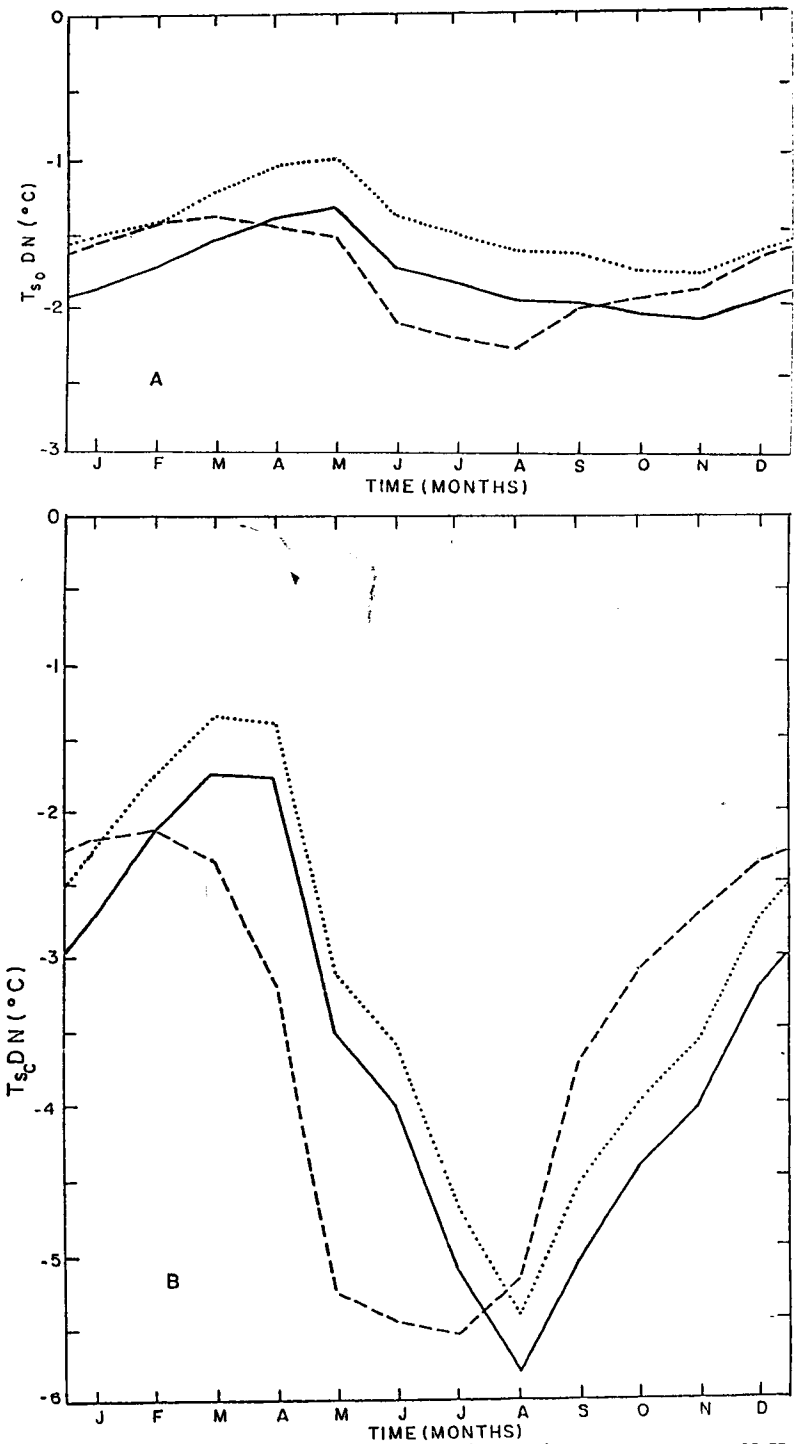

Figure 14. The average N. H. computed surface ocean temperature (Part A), and the average N H. surface toninental ground temperature (Part B), for 18 kyr BP. The continuous lines correspond to the solution in which anomalies of insolation, ice sheets and the decrease of the atmospheric CO_2 are included. The dashed lines correspond to the case when insolation anomalies are neglected; and the dotted line, to the case when the decrease of CO_2 is neglected.

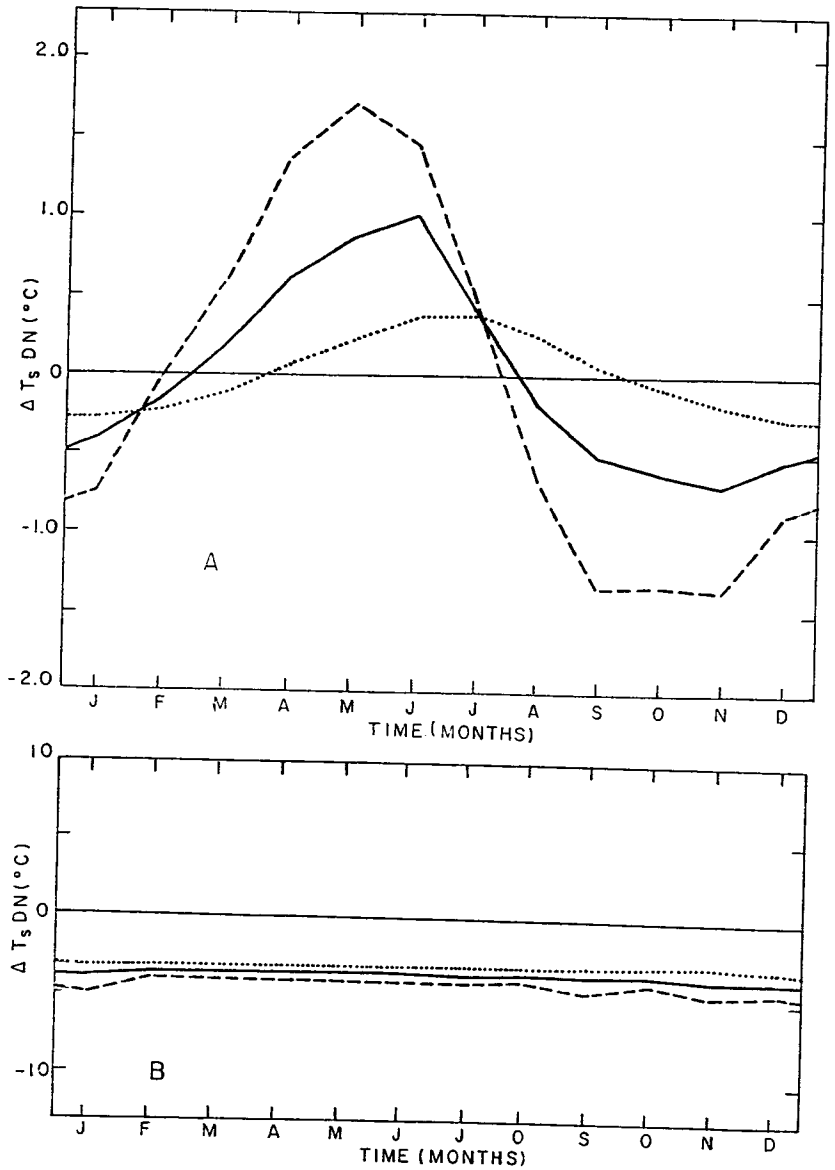

Figure 15. The net effect of the anomalies of insolation (part A) and of the atmospheric CO_2 decrease (Part B), for 18 kyr BP. The continuous, dashed and dotted lines correspond to the average increase of the ground surface temperature anomalies for the N. H., the N. H. continents and N. H. oceans respectively.

and of its net effect in the temperature anomaly are negligibly small, the net effect of IDN in the annual cycle of T_sDN is to decrease the negative anomaly in Spring and to increase it in the Fall, in an important way.

Fig. 15B shows the net effect of the decrease of atmospheric CO_2 in the N. H. average surface temperature anomaly (continuous line), in the N. H. average continental ground temperature anomaly (dashed line) and in the N. H. average surface ocean temperature anomaly. The net effect is the same during the whole year, and is equal to an increase of 0.3, 0.5 and 0.4°C in the magnitude of the negative temperature anomalies over oceans, continents and both oceans and continents respectively.

5. The ocean temperature anomalies and their effect in the continental climates

As mentioned in the introduction, in the experiments reported here, as well as in Adem (1985), the ocean temperature is included as a variable. To determine how realistic this computed anomalies

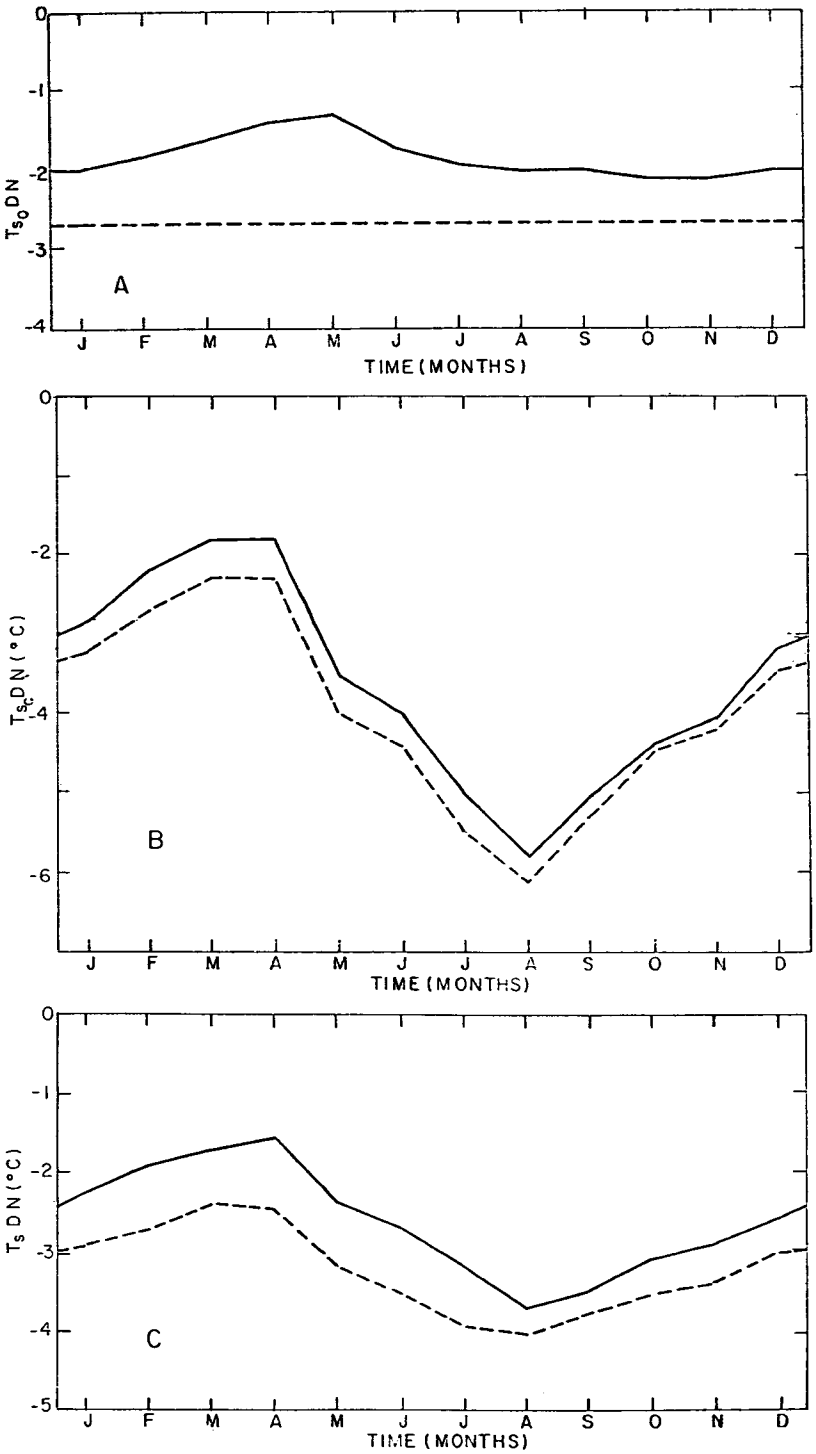

Figure 16. The Northern Hemisphere average surface temperature anomalies for 18 kyr BP when the ocean temperature anomalies are prescribed as given by CLIMAP (1976) (dashed lines) and when they are computed by the model (continuous lines). Part A is the average ocean temperature anomaly, Part B the average continental ground temperature anomaly and Part C the Northern Hemisphere ground temperature anomaly.

are and their effect in the continental climates we have carried out an experiment for 18 kyr BP, in which the ocean temperatures for July, as given by CLIMAP (1976), are prescribed and fixed during the whole year as in a previous experiment (Adem 1981), except that now the effect of CO_2 is included, and the most recent version of the model is used, in which the conservation of water vapor is included (Adem and Garduño, 1984). Due to the modifications in the heating functions there are some differences in the results. However they are essentially the same and for the purpose of this investigation, such differences are irrelevant. The new version of the model includes, besides the conservation of water vapor, a parameterization of the heating by radiation, which allows to vary the atmospheric CO_2 content in the computations (Adem and Garduño, 1984).

Fig. 16 shows the average surface temperature anomalies when the ocean temperatures are prescribed (dashed line) and when they are computed (continuous line). The ordinate, in part A is the average sea surface temperature anomaly, in part B the average continental ground temperature, and in part C, the average Northern Hemisphere ground temperature anomaly (oceans and continents). The abscissa is the time of the year in months.

Comparison of the continuous and dashed curves in 16A shows that the computed sea surface temperature anomalies are of smaller magnitude than those given by CLIMAP (1976). The annual average computed by the model is equal to -1.8^oC whose absolute value is 0.9^oC smaller than the average value given by CLIMAP (1976). The model has generated about two thirds of the anomaly which can, therefore, be attributed to the combined effect of the existence of the ice sheets, the decrease of atmospheric CO_2 and the anomalies of insolation due to the orbital variation.

Comparison of the continuous and dashed curves in 16B shows that the effect of computing a sea surface temperature anomaly with an annual average whose absolute value is 0.9^oC smaller than the CLIMAP (1976) values, has a smaller difference in the continents, where the annual computed average ground temperature anomaly is of about -3.6^oC. The absolute value of this average is 0.4^oC smaller than the one for the case when CLIMAP values are used in the ocean.

Fig. 16C shows that for the whole region of integration, the model with the computed ocean temperature anomalies has reproduced a large percentage of the average ground temperature anomaly, with an annual average of -2.6^oC whose absolute value is 0.7^oC smaller than the value obtained when the ocean temperature anomalies are prescribed.

6. General remarks and conclusions

The above results should be considered preliminary in nature and subject to revision when more realistic models become available. An attempt has been made to include as a variable the surface ocean temperature anomalies, with a very simplified model. From the results for 18 kyr BP shown in the previous section (Fig. 16B) it appears that the absolute values of computed negative anomalies are smaller than those obtained by CLIMAP (1976). This could be due to the simplification of the model. An improvement could possibly be obtained by using a more sophisticated model, with improved parameterizations of the heating components and of the transports by winds and by ocean currents. Improvements could also be obtained by improving the temperature snow-ice feedback mecanism.

Another improvement is expected by refining the physics for the computations of the atmospheric CO_2 effect. In fact, the model used in these experiments yields a Northern Hemisphere increase of 1.0^oC corresponding to the experiment of doubling the atmospheric CO_2 (Adem and Garduño,

1984), which is lower than the values obtained by most of the General Circulation Models.

Therefore it is expected that an improved treatment of the CO_2 effect, would produce bigger negative temperature anomalies, which would raise the effect from the 0.4 decrease obtained in the present computations to about 1.0°C. This would reduce considerably the discrepancies of the computed values of surface ocean temperatures and the CLIMAP (1976) values for 18 kyr BP.

For the case when CLIMAP (1976) ocean temperature values are used, the computed surface temperature values over the continents for 18 kyr BP have been compared in a previous paper (Adem 1981a) with those obtained in some localities by analysis of fossil pollen and other periglacial evidence, showing a relative good agreement, which is also valid for the corresponding values computed in this paper.

Acknowledgements

I am indebted to Jorge Zintzún and René Garduño for assisting me with the programming and with the numerical computation and to José Lauro Ramírez for helping me with the preparation of the figures.

REFERENCES

Adem, J., 1981a. Numerical simulation of the annual cycle of climate during the ice ages. *J. Geophys. Res.*, **86**, 12015-12034.

Adem, J., 1981b. Numerical experiments on ice age climates. *Climatic Change*, **3**; 155-171.

Adem, J., 1982. Simulation of the annual cycle of climate with a thermodynamic numerical model. *Geofís. Int.*, **21**, 229-247.

Adem, J., 1985 The climate of ten thousand years ago: A numerical simulation. *Geofís. Int.*, **24** 383-407.

Adem, J. and R. Garduño, 1982. Preliminary experiments on the climatic effect of an increase of the atmospheric CO_2 using a thermodynamic model. *Geofís. Int.*, **21**, 309-324.

Adem, J. and R. Garduño, 1984. Sensitivity studies on the climatic effect of an increase of atmospheric CO_2. *Geofís. Int.* **23**, 17-35.

Adem, J., A. Berger, P. Gaspar, P. Pestiaux and J. P. van Ypersele, 1984. Preliminary results on the simulation of climate during the last deglaciation with a thermodynamic model. A. L. Berger *et al.* (eds.). Milankovitch and Climate. Part 2, 527-537, D. Reidel Publishing Company.

Alyea, F. M., 1972. Numerical simulation of an ice-age paleo-climate. Atmos. Sci. Pap. No. 193. Colorado State University 134 pp. (Available from NTIS, PB232823/5, or from Xerox University Microfilms, Ann Arbor, No. 72-13022).

Berger, A., 1978. Long-term variations of daily insolation and Quaternary climate changes. *J. Atmos. Sci.*, **35**, 12, 2362-2367.

CLIMAP, 1976. The surface of the ice-age earth. *Science*, **191**, 1131-1137.

Denton, G. H. and T. J. Hughes, 1981. The last great ice sheets. J. Wiley, New York.

Gates, W. L., 1976a. Modeling the ice-age climate. *Science*, **191**, 1138-1144.

Gates, W. L., 1976b. The numerical simulation of ice-age climate with a global general circulation model. *Atmos. Sci.*, **33**, 1844-1873.

Hastenrath, S. and J. E. Kutzbach, 1983. Paleoclimatic estimates from water and energy budgets of East African lakes. *Quaternary Res.*, **19**, 141-153.

Hastenrath, S. and J. E. Kutzbach, 1985. Late pleistocene climate and water budget of the South American Altiplano. *Quaternary Res.*, **24**, 249-256.

Kutzbach, J. E., 1983a. Monsoon rains of the late Pleistocene and early Holocene: Patterns, intensity and possible causes of changes. In variations in the global water budget (A. Street-Perrott *et al.* (eds), pp. 371-389. Reidel Publishing Company.

Kutzbach, J. E., 1983b. Modeling of Holocene climates 1983. "Late Quaternary Environments of the United States", Vol. 2. "The Holocene" (H. E. Wright, Jr., ed.), Univ. of Minn. Press., pp. 271-277.

Kutzbach, J. E. and B. L. Otto-Bliesner, 1982. The sensitivity of the African-Asian monsoonal climate to orbital changes for 9 000 years B. P. in a low-resolution general circulation model. *J. Atmos. Sci.*, **39**, 1177-1188.

Kutzbach, J. E. and P. J. Guetter, 1984a. Sensitivity of late-Glacial and Holocene climates to the combined effects of orbital parameters changes and lower boundary condition changes:"Snapshot" simulations with a General Circulation Model for 18, 9 and 6 Ka BP *Ann. Glaciol.* **5**, 85-87.

Kutzbach, J. E. and P. J. Guetter, 1984b. The sensitivity of monsoon climates to orbital parameter changes for 9 000 years BP: Experiments with the NCAR General Circulation Model. In "Milankovitch and Climate". A. L. Berger *et al.* (eds.). Part 2, pp. 801-820. Reidel, Dordrecht.

Kutzbach, J. E. and F. A. Street-Perrot, 1985. Milankovitch forcing of fluctuations in the level of tropical lakes from 18 to 0 kyr B P. *Nature,* **317**, 130-134.

Kutzbach, J. E. and H. E. Wright, Jr., 1985. Simulation of the climates of 18 000 years B P: Results for the North American/North Atlantic/European Sector and comparison with the geologic record of North America. *Quaternary Science Reviews,* **4**, 147-187.

Kutzbach, J. E. and P. J. Guetter, 1986. The influence of changing orbital parameters and surface boundary conditions with climate simulation for the past 18 000 years. *J. Atmos. Sci.,* **43**, 1726-1759.

Manabe, S. and D. G. Hahn, 1977. Simulation of the tropical climate of an Ice Age. *J. Geophys. Res.,* **82** 3889-3911.

Neftel, A., H. Oescher, J. Schwander, B. Stauffer and R. Zumbrunn, 1982. Ice core sample measurements give atmospheric CO_2 content during the past 40 000 years. *Nature,* **295**, 220-223.

Newell, R. E. and G. F. Herman, 1975. Diagnostic studies of the past ice age. Proc. WMO/IAMAP *Symp. Long-Term Climatic Fluctuations,* No. 421 WMO, Geneva, 239-300.

Saltzman, B. and A. D. Vernekar, 1975. A solution for the Northern Hemisphere climatic zonation during a glacial maximum. *Quat. Res.* **5**, 307-320.

Swain, A. M., J. E. Kutzbach and S. Hastenrath, 1983. Estimates of holocene precipitation for Rajasthan, India, Based in pollen and lake-level data. *Quat. Res.* **19**, 1-17.

Williams, J., R. G. Barry and W. M. Washington, 1974. Simulation of the atmospheric circulation using the NCAR global circulation model with ice age boundary conditions. *J. Appl. Meteor.* **13**, 305-317.

Winkler, M. G., A. M. Swain and J. E. Kutzbach, 1986. Middle Holocene dry period in the Northern Midwestern United States: Lake levels and pollen stratigraphy. *Quat. Res.* **25**, 235-250.